ELSEVIER

Biochemical Pharmacology 65 (2003) 447–456

Biochemical Pharmacology

www.elsevier.com/locate/biochempharm

Probing the binding of the flavonoid, quercetin to human serum albumin by circular dichroism, electronic absorption spectroscopy and molecular modelling methods

Ferenc Zsila*, Zsolt Bikádi, Miklós Simonyi

Department of Molecular Pharmacology, Institute of Chemistry, Chemical Research Center, P.O. Box 17, Budapest H-1525, Hungary

Received 26 August 2002; accepted 10 October 2002

Abstract

The plant derived flavonoid compound quercetin, possesses wide range of biological activities in the human body by interacting with nucleic acids, enzymes and other proteins. As has recently been shown this molecule of polyphenolic type extensively binds to human serum albumin (HSA), the most abundant carrier protein in the blood. Electronic absorption, circular dichroism (CD) spectroscopy and molecular modelling methods were used to characterize optical properties of the quercetin–HSA complex, and to gain information on the binding mechanism at molecular level. The red shift and hypochromism of the longest-wavelength absorption band of quercetin relative to the spectral properties in ethanol suggests that one or more phenolic OH groups of the bound ligand is ionized and that the exocyclic phenyl ring is not coplanar with the benzopyrone moiety. It was found that quercetin shows extrinsic optical activity on interaction with HSA. The induced CD spectra were utilized to calculate the association constant at 37° ($1.46 \pm 0.21 \times 10^4$ M^{-1}) and to probe the ligand binding site. Results of the CD displacement experiments performed with palmitic acid and salicylate were interpreted together with the findings of molecular modelling calculation performed on the quercetin–HSA complex. Computational mapping of possible binding sites of quercetin revealed the molecule to be bound in the large hydrophobic cavity of subdomain IIA. The protein microenvironment of this site was found to be rich in polar (basic) amino acid residues which are able to help to stabilize the negatively charged ligand bound in non-planar conformation. Additionally, the position of quercetin within the binding pocket allows simultaneous binding of other ligands such as warfarin, or sodium salycilate.

Keywords: Quercetin; Human serum albumin; Ligand binding; Circular dichroism; Induced chirality

1. Introduction

Quercetin (3,5,7,3′,4′-pentahydroxyflavone; Fig. 1) is a member of naturally occurring widely distributed compounds, the flavonoids, which are ubiquitous phenolic secondary metabolites found in plants, fruits, flowers and plant derived foods [1]. Flavonoids consist of two aromatic rings (A and B in Fig. 1) linked by an oxygen-containing heterocycle (ring C). Abundant in the human diet, quercetin with potent antioxidant and metal ion chelating capacity, possesses various biological and biochemical effects including anti-inflammatory, antineoplastic and cardiprotective activities [2,3]. Additionally, quercetin is among the group of phytoestrogens (plant derived molecules with estrogenic or anti-estrogenic effects) suggested to reduce risks of certain cancers [4]. A full understanding of the modes of action of bioflavonoids, however, requires the study of their interactions with all possible biological targets, including nucleic acids [5], enzymes [6,7] and other proteins [8].

Serum albumin as one of the most abundant carrier proteins plays an important role in the transport and disposition of endogenous and exogenous ligands present in blood [9]. Distribution and metabolism of many biologically active compounds (drugs, natural products, etc.) in the body are correlated with their affinities towards serum albumin. Thus, the investigation of such molecules with respect to albumin binding is imperative and of fundamental importance. It has recently been proved that serum

* Corresponding author. Fax: +36-1-325-7750.
E-mail address: zsferi@chemres.hu (F. Zsila).
Abbreviations: AM1, Austin Method 1; CD, circular dichroism; CE, Cotton effect; HSA, human serum albumin; L/P, Ligand/protein molar ratio.

0006-2952/02/$ – see front matter
PII: S0006-2952(02)01521-6

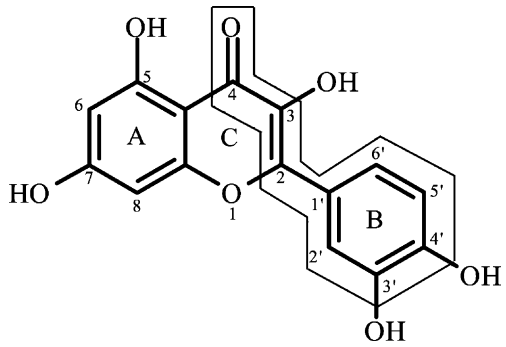

Fig. 1. Chemical structure of quercetin. Frame highlights the cinnamoyl part of the molecule.

albumin plays decisive role in the transport and disposition of flavonoids, especially of quercetin [8,10]. Using radiolabelled ligand in an ultracentrifugation assay, quercetin was suggested to bind to one of the major primary drug binding sites termed Site I in the IIA subdomain of HSA with an association constant of $267 \pm 33 \times 10^3$ M^{-1} at 20° [11]. The non-steroid anti-inflammatory drug ibuprofen, a marker ligand for the other primary drug binding site (Site II within the subdomain IIIA) was shown to be unable to displace radiolabelled quercetin from HSA [11]. Contrary to this, it was concluded from fluorescence energy transfer measurements of the 3-hydroxyflavone–HSA complex that this flavonoid binds to high and low affinity sites located in the IIIA and IIA subdomain, respectively [12].

The strong bathochromic shift observed in the absorption spectrum of flavonoids upon complexation with HSA provides a good starting point to study the complex by absorption spectroscopy [10]. Since quercetin is optically inactive, it can be expected that its binding to the chiral host (albumin) leads to the appearance of induced chirality [13]. Accordingly to this assumption we applied CD and electronic absorption spectroscopy to characterize the optical properties of the quercetin–HSA complex. To our knowledge this is the first report on induced optical activity due to flavonoid–protein interaction pointing out the value of CD spectroscopy in studying this biologically significant field. Utilizing the induced circular dichroism spectra, the association constant of quercetin was calculated at 37° and its binding location was studied in displacement experiments using ligands with known binding sites on HSA. Experimental observations were interpreted on the basis of molecular modelling calculations performed for the quercetin–HSA complex.

2. Experimental

2.1. Materials

Essentially fatty acid-free human serum albumin (Lot no. 14H9319, 96% purity), quercetin dihydrate (Lot no. 01912KV-042, 98.9% purity) and palmitic acid were purchased from Sigma-Aldrich Co., and used as supplied. Double distilled water and HPLC grade ethanol (Chemolab, Hungary) were used. All other chemicals were analytical grade.

Quercetin was dissolved in ethanol purged with nitrogen to obtain 2.90×10^{-3} M stock solution. Ringer buffer pH 7.4 containing 137 mM NaCl, 2.7 mM KCl, 0.8 mM $CaCl_2$, 1.1 mM $MgCl_2$, 1.5 mM KH_2PO_4 and 8.1 mM $Na_2HPO_4 \cdot 12H_2O$ was used to prepare HSA stock solution (1.0×10^{-4} M). Albumin concentration was obtained by measuring absorbance at 279 nm with the value of $E_{1\ cm}^{1\%} = 5.31$ [14]. A molecular weight of 66,500 was used for HSA.

2.2. Electronic absorption and CD measurements

CD and ultraviolet-visible (UV/Vis) spectra were recorded on a Jasco J-715 spectropolarimeter at $37 \pm 0.2°$ in a rectangular cuvette with 1 cm pathlength. Temperature control was provided by a Peltier thermostat equipped with magnetic stirring. The spectra were accumulated four times with a bandwidth of 1.0 nm and a resolution of 0.2 nm at a scan speed of 100 nm/min. Induced CD spectra were obtained as the CD of quercetin–HSA mixture minus the CD of HSA alone at the same wavelengths and is expressed as ellipticity in millidegrees.

2.3. Measuring the CD/UV/Vis spectra of quercetin–HSA complex

Between 290 and 500 nm, a 1 cm cuvette was filled with 2 mL 1×10^{-4} M HSA solution. After recording the CD and absorbance spectra of HSA, 5 μL aliquots of quercetin stock solution was added consecutively. Thirteen spectra were taken between 0.07 and 0.94 quercetin/HSA molar ratios.

2.4. CD/UV/Vis titration of HSA with quercetin between 290 and 380 nm to collect data for the calculation of the association constant

A cuvette of 1 cm was filled with 2 mL 1×10^{-4} M HSA solution. After recording the CD and absorbance spectra of HSA 5 μL volumes of quercetin stock solution were added consecutively. Twenty-three spectra were taken in the range of 0.07–1.67 quercetin/HSA molar ratios and the CD values in millidegree were taken at 308 nm.

2.5. Calculation of the association constant of quercetin–HSA complex

The stereospecific interaction between a ligand (L) and its primary site on the protein (P) may be quantified by the association constant (K_a):

$$L + P = LP; \quad K_a = \frac{[LP]}{[L][P]} \tag{1}$$

It is evident that

$$[L] = c_L - [LP] \quad (2)$$

and

$$[P] = c_P - [LP] \quad (3)$$

where c_L and c_P mean the total concentrations of the ligand and protein, respectively. Assuming that the quercetin–HSA complex (1:1 stoichiometry) is responsible for the induced CD band, it can be written that

$$CD_{308\ nm}\,(mdeg) = k[LP] \quad (4)$$

where $k = 32982.1\ \Delta\varepsilon l$ ($\Delta\varepsilon$ is the extrinsic molar optical activity at 308 nm of quercetin bound to HSA in $M^{-1}\ cm^{-1}$ and l is the optical pathlength in cm).

Using Eqs. (1)–(4), we obtain

$$CD\,(mdeg) = \frac{k}{2}(c_P + c_L + K_a^{-1} - \sqrt{(c_P + c_L + K_a^{-1})^2 - 4c_P c_L}) \quad (5)$$

In order to calculate the optimal values of k and K_a, non-linear regression analysis method was applied (NLREG® statistical analysis program, version 3.4). The values of K_a and k were obtained to be $1.46 \pm 0.21 \times 10^4$ and $3.28 \times 10^5\ M^{-1}$ at pH 7.4 ($r^2 = 0.998$); $\Delta\varepsilon_{308\,nm} \approx -10\ M^{-1}\ cm^{-1}$.

2.6. Molecular modelling calculations

The AutoDock program package was used to locate possible quercetin binding sites on the HSA molecule. The three-dimensional coordinates of human serum albumin were obtained from the Protein Data Bank (entry PDB code 1AO6). Grid maps were generated with 0.375 Å spacing by the AutoGrid program for the whole protein target. 12-10 and 12-6 Lennard–Jones parameters (supplied with the program package) were used for modelling H-bonds and van der Waals interactions, respectively. The Lamarckian genetic algorithm (LGA) and the pseudo-Solis and Wets methods were applied for minimisation using default parameters. Random starting positions on the entire protein surface, random orientations and torsions were used for the ligand. All computer modelling procedures were run on a Silicon Graphics Octane workstation under Irix 6.5 operation system.

3. Results and discussion

3.1. Electronic absorption spectrum of quercetin in ethanol and in buffer solution

The UV/visible spectrum of quercetin, illustrated in Fig. 2, was obtained using ethanol as the common solvent of flavonoids. Inserted are the experimental λ_{max} values, together with molar absorption coefficients (ε in $M^{-1}\ cm^{-1}$) for all clearly identifiable absorption bands above 215 nm. In the spectral range of 240–450 nm flavone and their hydroxy substituted derivatives show two main absorption bands commonly referred to as Band I (300–400 nm) and Band II (240–280 nm) [15]. Band I is supposed to be associated with the light absorption of the cinnamoyl system (B + C ring), and Band II with the

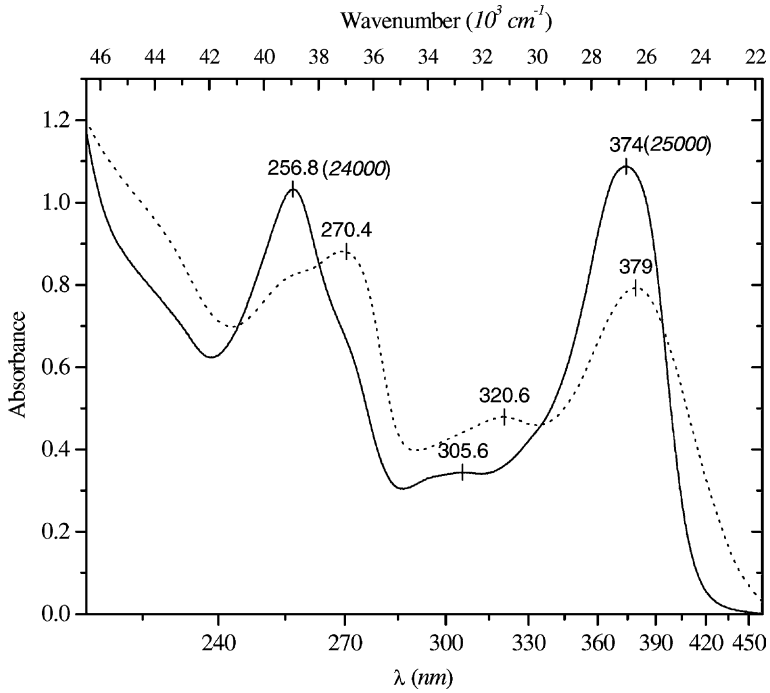

Fig. 2. Electronic absorption spectrum of quercetin in ethanol (solid line) and in pH 7.4 Ringer buffer (dotted line) between 215 and 460 nm at room temperature ($l = 1$ cm; $c = 4.29 \times 10^{-5}$ M). Molar absorption coefficients ($M^{-1}\ cm^{-1}$) are italicized.

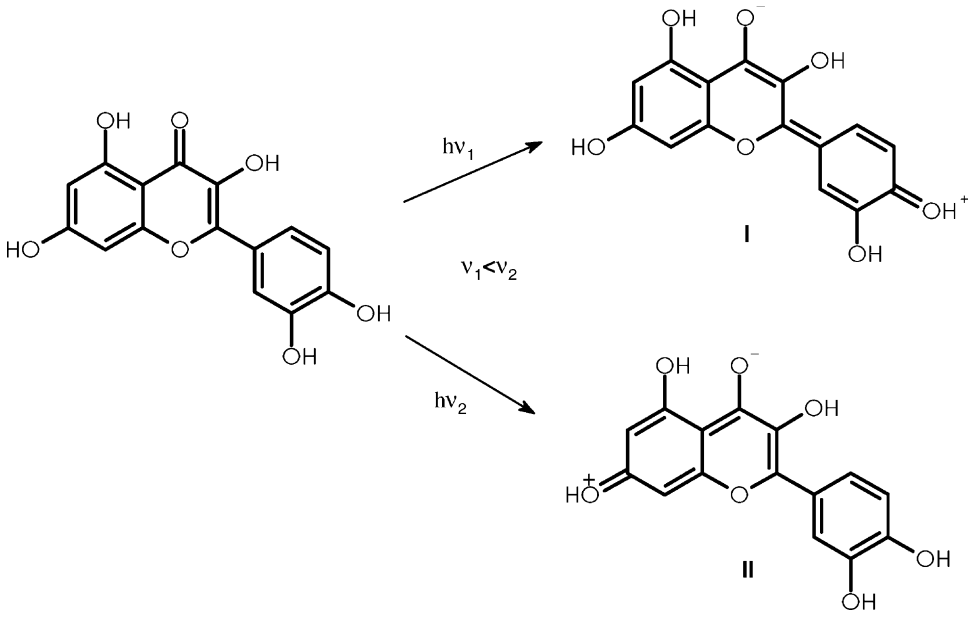

Fig. 3. Mesomeric structure illustration of the excited states of quercetin.

absorption of the benzoyl moiety formed by the A + B ring (Fig. 1). These transitions are π–π^* in nature and, in a first approximation, can be represented by two resonance structures depicted in Fig. 3 [16,17]. The zwitterionic or charge separated forms represent the excited states; both transitions are electronically allowed as can be inferred from their large ε values (Fig. 2). Band I of quercetin at 374 nm consists of at least two sub-bands at around 387 and 367 nm as shown by the second derivative of the spectrum. The origin of these sub-bands are less clear, i.e., they might be energetically close lying singlet transitions [16] or vibrational sub-bands. The width of Band I at the half of the absorption maximum is 4054.7 cm^{-1}. Wavelength positions and intensities of Bands I and II are sensitive to the substituents of rings A and B [15]; hydroxyl group(s) on ring B (especially at 4′-position) shifts Band I to longer wavelengths but affects Band II only slightly. Upon increasing number of hydroxyl groups in ring A (i.e., 5-OH) Band II becomes more pronounced and is shifted to higher wavelengths. It is important to note that the ionization of the OH groups causes strong bathochromic shift of all absorption bands [15]. For example, rutin (3-rhamnosylglucoside of quercetin) shows two principal absorption bands at 259 and 359 nm in methanol, which are red-shifted to 271 and 393 nm due to the addition of sodium acetate [15]. The most acidic phenolic OH groups of quercetin are in the 3, 7 and 4′ positions [15,18], which are dissociated at physiological pH though this process is far from being complete and results in a mixture of neutral and anionic species [6]. The characteristics of the absorption spectrum taken in buffer solution pH 7.4 correspond well to this situation showing moderate red shift and significant broadening of Bands I and II (Fig. 2). Ionized forms of quercetin have absorption bands at higher wavelengths but due to the coexistence of neutral molecules absorbing energy at lower wavelengths the two kinds of absorption spectra fuse resulting in the sum curve of Fig. 2 [6]. The weak, electronic dipole forbidden but magnetically allowed n $\rightarrow$ π^* transition of the carbonyl moiety is located under the intense Band I presumably between 340 and 375 nm [19]. The ^1L_b transitions of the hydroxyl-containing aromatic rings appear between Bands I and II around 305 nm characterized by suppressed vibrational fine structure.

3.2. Electronic absorption spectrum of quercetin bound to HSA at pH 7.4 between 290 and 500 nm

Quercetin was added progressively to the 1.0×10^{-4} M fatty acid-free HSA solution (Ringer buffer, pH 7.4) to achieve ligand/protein ratios from 0.07 to 0.94 and absorption spectra were registered between 290 and 500 nm (at this concentration, light absorption of albumin does not allow spectrum measurements below 290 nm). Selected spectra of HSA-bound quercetin (spectra of quercetin–HSA complex minus the absorption curve of albumin alone) are shown in Fig. 4 together with the spectrum of quercetin taken in ethanol. The comparison of these curves demonstrates that protein binding causes a strong bathochromic shift (30 nm) of Band I which suggests the presence of a specific interaction between the ligand and its binding environment. As mentioned earlier, deprotonation of phenolic OH substituents leads to a bathochromic shift due to the extension of π conjugation. Besides, Band I shows significant broadening in the presence of HSA; at 0.29 ligand/protein (L/P) ratio the half-bandwidth is 5306 cm^{-1} which is more than 1000 cm^{-1} larger relative to that measured in ethanol. It is well known that molecules

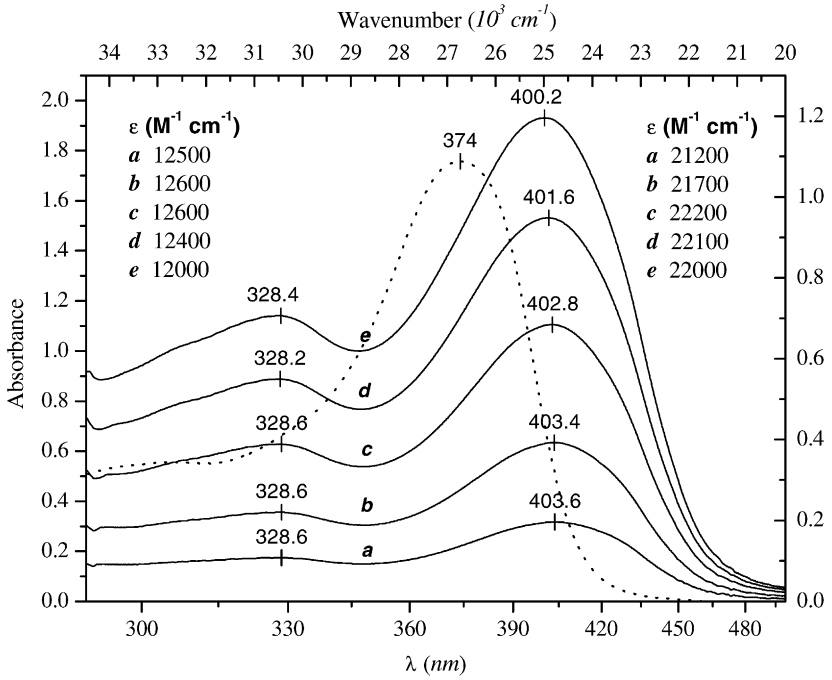

Fig. 4. Absorption spectra of quercetin in ethanol (dotted line, left axis) and bound to HSA (solid lines, right axis) between 290 and 500 nm in Ringer buffer, pH 7.4 at 37°. The quercetin/albumin molar ratios were: 0.14:1 (curve a), 0.30:1 (curve b), 0.51:1 (curve c), 0.72:1 (curve d) and 0.94:1 (curve e). Molar absorption coefficients (ε) are shown corresponding to the denoted wavelengths.

show narrow absorption bands or separate lines in the gas phase due to the absence of intermolecular interactions. On the other hand, in dissolved state solute–solvent interactions cause notable band broadening. The stronger and more numerous these interactions are (dispersion → dipole−dipole → H-bond → ionic) the greater changes occur in the absorption band-shape, position and intensity. Accordingly, the band broadening of quercetin can be interpreted as a consequence of its specific, non-covalent interactions with the amino acid residues of the binding site. The intensity of Band I is also altered; the values of the molar absorption coefficients are moderately decreased upon albumin binding (Fig. 4, cf. Fig. 2). Since the absorption band-shape is also changed, it is more reliable to compare the corresponding oscillator strengths (f) calculated by integrating the area under Band I. For Band I $f = 0.502$ and 0.442 were obtained in EtOH and in quercetin–HSA solution (L/P = 0.29), respectively. Despite of the hypochromism of Band I, red shifted ^1L_b band of the quercetin benzene rings at 328 nm shows enhanced intensity (hyperchromism, Fig. 4). Different behaviour of these transitions stem from their distinct localization on the chromophoric system. The π–π* excitation of Band I involves the π-systems of both B- and C-rings. These rings are connected by a single C–C bond (Fig. 1) around which rotation can occur resulting in the decrease of conjugation between the two rings. Reduced planarity leads to the fall of intensity of Band I [15, p. 93–94,20]. It is reasonable to assume that accommodation of quercetin to its binding site on HSA might necessitate such conformational change. In spite of this, the binding site is not able to distort the rigid and planar benzene rings of quercetin so their π orbitals involved in the ^1L_b transitions remain sterically unaltered. In order to estimate the extent of the rotation around the C_2–$C_{1'}$ bond a simple calculation can be performed [20]: $\cos\Theta/\cos\Theta_0 = f/f_0$ where Θ and Θ_0 are the angles between the planes of the exocyclic phenyl ring and the C-ring in the HSA bound and free quercetin molecules, respectively, and f and f_0 are the corresponding oscillator strengths of Band I. It is worth to mention that in solid state the B-ring is almost planar ($\Theta = 7°$) with respect to the rest of the molecule [21]. In solution, however, where the crystal packing forces are absent different conformations might exist. In agreement with literature data [22] our semi-empirical (AM1) quantum chemical calculation showed that the B-ring deviates with 27° from planarity due to van der Waals distance violation between *ortho* hydrogens of ring B and the C_3 hydroxyl group. Using the values of oscillator strengths calculated above, we obtain $\Theta \approx 40°$ in the albumin-bound quercetin molecule ($\Theta_0 = 27°$).

3.3. Circular dichroism spectrum of the quercetin–HSA complex

CD bands appear in the wavelength range of the absorption of a given compound. The absorption bands of quercetin, as discussed above, allows to anticipate the appearance of at least three induced CD bands when quercetin is bound to the asymmetric albumin environment. Experimentally, fatty acid-free HSA induces three, negative–positive–negative CD bands in the region from

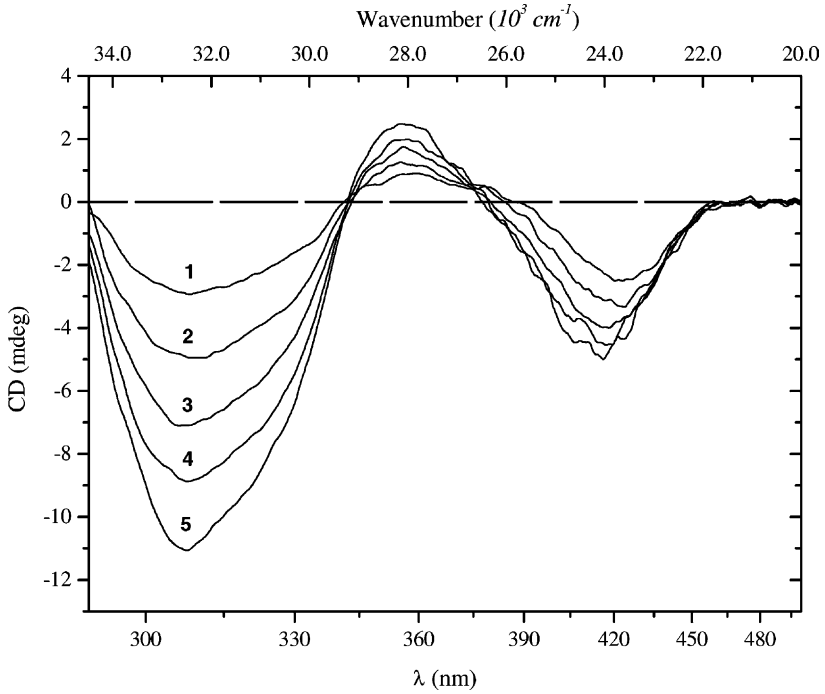

Fig. 5. UV-Vis range of CD spectra for quercetin–HSA complexes in Ringer buffer, pH 7.4 at 37°. Different quercetin/albumin molar ratios were: 0.22:1 (curve 1), 0.36:1 (curve 2), 051:1 (curve 3), 0.65:1 (curve 4) and 0.80:1 (curve 5). $c_{HSA} = 1 \times 10^{-4}$ M.

290 to 500 nm (Fig. 5). Table 1 summarizes band positions and the intensities for all L/P ratios used in the CD measurements, expressed as molar dichroic absorption coefficients ($\Delta\varepsilon$) in M^{-1} cm^{-1} calculated with respect to total quercetin concentration. The longest wavelength CE around 417 nm is tentatively assigned to the red shifted $n \rightarrow \pi^*$ transition of quercetin [19]. This band carries hidden vibronic fine structure revealed by computer deconvolution (data not shown) which is characteristic to $n \rightarrow \pi^*$ transitions. The stronger negative band at 308 nm probably arises from the asymmetrically perturbed ^1L_b excitation of the benzene chromophores. The origin of the small positive CE at 357 nm is unclear. The overall shape of the CD spectrum was not affected at higher L/P molar ratios. Since there is no sign of intermolecular interaction in the CD spectra (i.e., exciton coupling [23]), it can be concluded that quercetin binds to HSA in monomeric form. Thus, the induced CD spectrum was utilized to achieve two goals: (i) probing the location of quercetin binding site on HSA and (ii) calculating the association constant (K_a).

Table 1
Intensities ($\Delta\varepsilon$ in M^{-1} cm^{-1}) and wavelength positions (λ in nm) of the induced CD bands of quercetin at different ligand/protein ratios calculated with respect to the total quercetin in the solutions

L/P ratio	$\Delta\varepsilon_1$ (λ)	$\Delta\varepsilon_2$ (λ)	$\Delta\varepsilon_3$ (λ)
0.14	−3.9 (311.8)	+1.6 (355.6)	−4.2 (425.6)
0.22	−4.1 (308.2)	+1.3 (359)	−3.5 (423.2)
0.30	−4.3 (307.8)	+1.1 (360.2)	−3.1 (423.8)
0.36	−4.2 (308.6)	+1.1 (355.2)	−2.8 (423.6)
0.43	−4.3 (308)	+0.9 (356.4)	−2.6 (417.8)
0.51	−4.3 (306.2)	+1.1 (356)	−2.4 (418.2)
0.58	−4.3 (308.4)	+0.9 (354.2)	−2.2 (417.2)
0.65	−4.2 (307.8)	+0.9 (357.2)	−2.2 (417.2)
0.72	−4.3 (308.6)	+0.9 (360.2)	−2.1 (412)
0.80	−4.3 (307.8)	+1.0 (355.2)	−1.9 (416.2)
0.87	−4.1 (307.6)	+1.0 (354.8)	−1.8 (418.2)
0.94	−4.1 (307.8)	+0.9 (356.4)	−1.5 (417.8)

It seemed reasonable to investigate quercetin binding also in the presence of fatty acids which have five primary, crystallographically well defined binding sites on HSA. The IIIA subdomain contains two high affinity sites for long-chain fatty acids but, due to steric reasons, these molecules cannot be accommodated in the cavity of subdomain IIA [24]. Upon addition of palmitic acid to quercetin–HSA solution, the longest wavelength negative CE is intensified and shifts to higher energies by 10 nm (417 → 407 nm) while the position of the corresponding absorption band (Band I) remains unchanged though its intensity decreased (Fig. 6). Parallel with these modifications, the negative CD band at 307 nm is also slightly increased together with the ^1L_b absorption. Following from the above discussions on the absorption and CD spectra of the quercetin–HSA complex, these changes suggest that:

(a) Quercetin does not bind to the long-chain fatty acid sites of HSA (five primary sites in domains I and III). This result is in good agreement with the investigations of Boulton *et al.* who found that (±)-ibuprofen, the marker ligand of subdomain IIIA, did not displace quercetin from HSA [11].
(b) Palmitic acid enhances the binding of quercetin to HSA.

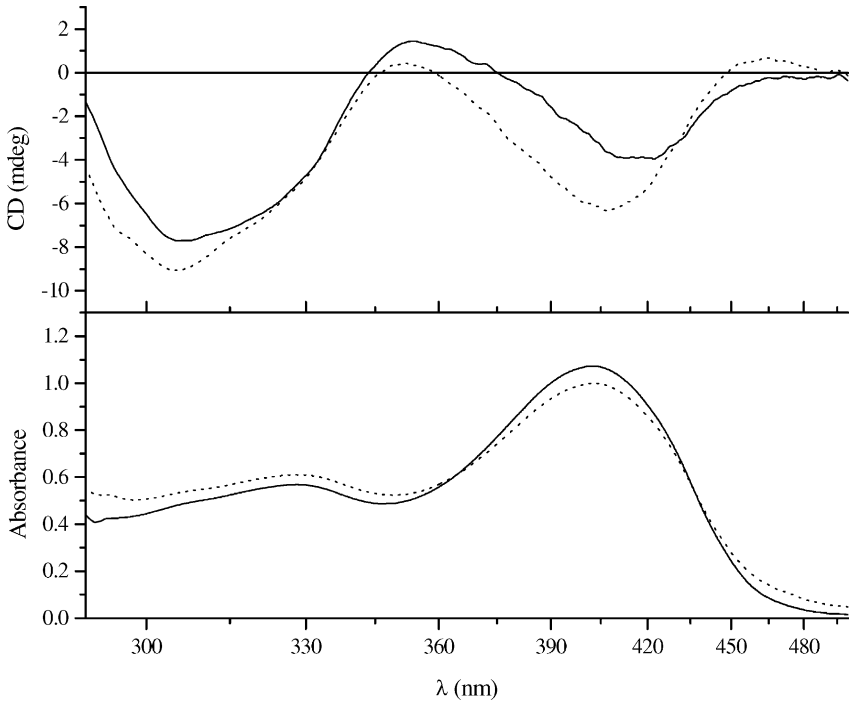

Fig. 6. Comparison of the induced CD spectra of quercetin–HSA complex in the absence and in the presence of palmitic acid. HSA:quercetin:palmitic acid 1:0.5:0 (solid line) and 1:0.5:2.5 (dotted line). $c_{HSA} = 9.1 \times 10^{-5}$ M; $c_{querc} = 4.7 \times 10^{-5}$ M; $c_{palm} = 2.3 \times 10^{-4}$ M.

It is important to note that the same phenomenon (b) was observed in the case of warfarin, the anticoagulant drug, which binds primarily to subdomain IIA (Site I) as proved by X-ray crystallography [25]. Unfortunately, warfarin and its derivatives bound to HSA show induced CD bands interfering with that of quercetin [13]. In this respect, salicylate is a better choice because it gives no CD bands above 330 nm. We found that salycilate, known to have moderate and equal affinity ($K_a = 1.9 \times 10^5$ M^{-1}) for drug binding Sites I and II of HSA [26], does not alter position and amplitude of the negative CE at 416 nm but slightly decreases the intensity of Band I in the absorption spectrum. The results obtained from the displacement experiments indicate that quercetin does not bind to subdomain

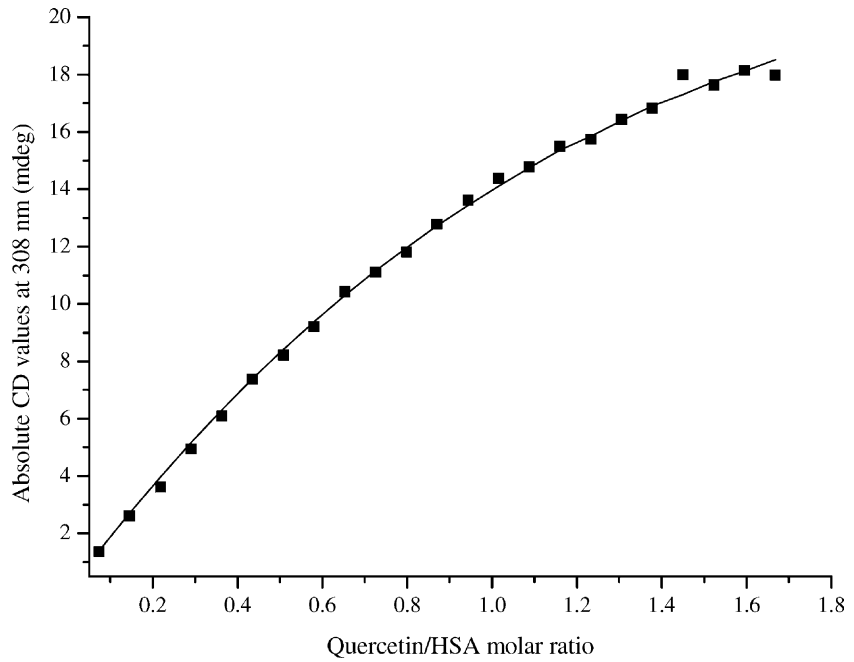

Fig. 7. CD titration of HSA with quercetin in a pH 7.4 Ringer buffer at 37°. CD intensities measured at 308 nm are plotted vs. the ligand/protein molar ratios. Squares: the experimental data. Solid line: the result of the curve fitting-procedure (non-linear regression analysis with 1:1 stoichiometry).

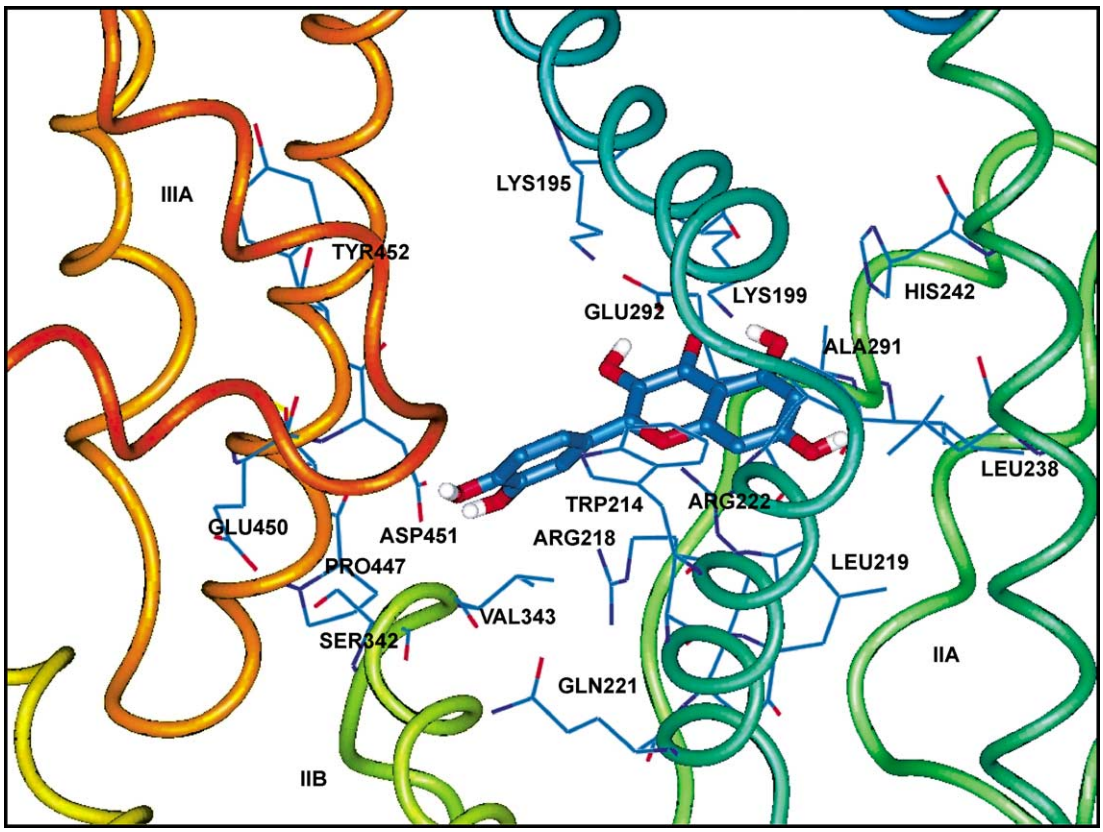

Fig. 8. Structural details of the interaction of quercetin with HSA obtained by molecular modelling method. Quercetin molecule is shown as cylinder model (C, blue; O, red; H, white). Amino acid residues of the binding pocket are denoted as wireframe models.

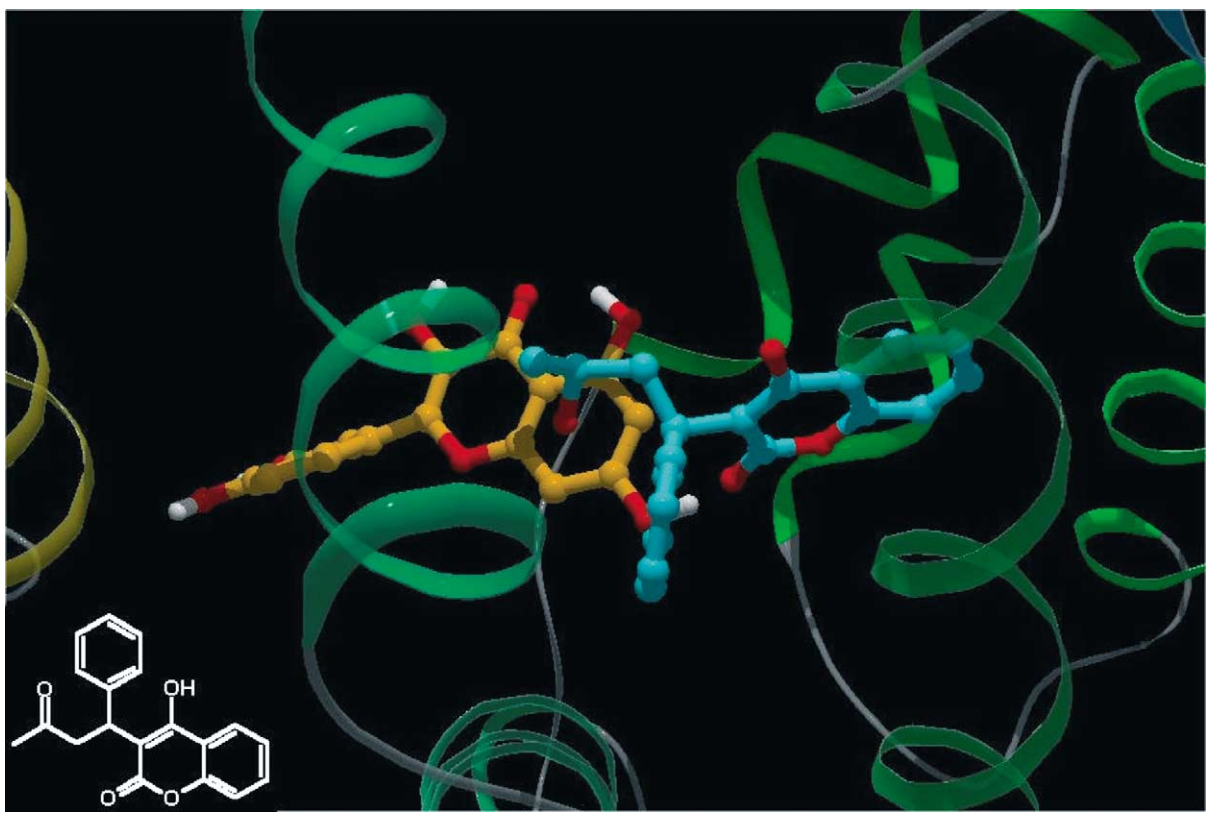

Fig. 9. Comparison of the mutual positions of quercetin (calculated by molecular modelling) and warfarin (X-ray, [25]) in the cavity of subdomain IIA. The ligands are shown as ball-and-stick models (orange: quercetin; light blue: warfarin). 2D structure of warfarin is depicted in the left-bottom comer.

IIIA, but rather to the hydrophobic cavity of subdomain IIA which is large enough to accommodate two ligand molecules explaining why salicylate moiety has no effect on the spectral properties of the quercetin–HSA complex.

The magnitude of negative CE at 308 nm was used to calculate the association constant of quercetin. To collect suitable amount of data, HSA was titrated with quercetin between 0.07 and 1.67 L/P ratios (Fig. 7). No significant intensity changes occurred after reaching the 1.45 L/P ratio. Applying non-linear regression analysis $1.46 \pm 0.21 \times 10^4\ M^{-1}$ was obtained for K_a at pH 7.4 ($t = 37^\circ$). This value is an order of magnitude smaller than $2.67 \pm 0.33 \times 10^5\ M^{-1}$ ($t = 20^\circ$) found by ultracentrifugation assay (estimated value for 37° was $1.77 \times 10^5\ M^{-1}$) [11]. The difference between these values is probably due to the different techniques by which they were obtained. The ultracentrifugation assay measures the overall binding while CD spectroscopy does not distinguish ligand molecules with different strengths of induced optical activity. Thus, it is possible that quercetin also has other binding site(s) on HSA besides Site I [12,27], and the K_a value obtained by CD spectroscopy belongs to the latter one, only.

3.4. Computational modelling of the quercetin–HSA complex

The crystal structure of HSA taken from the Protein Data Bank (entry PDB code 1AO6) was used to find the binding site of quercetin. The best energy ranked result is shown in Fig. 8. As can be seen, quercetin is situated within subdomain IIA in Sudlow's Site I formed by six helices. The benzopyrone moiety is located within the binding pocket but the B-ring protrudes from it and points toward the interface of IIB and IIIA subdomains. The A- and C-rings are practically coplanar, while ring B is rotated by 60° around the C_2–$C_{1'}$ bond. The interaction between quercetin and HSA is not exclusively hydrophobic in nature since there are several ionic (Lys195, Lys199, Arg218, Arg222, His242, Asp451, Glu292) and polar residues (Gln221, Tyr341, Ser342, Tyr452) in the proximity of the bound ligand (Table 2) playing important role in stabilizing the negatively charged quercetin molecule via H-bonds and electrostatic interactions. For instance, the nitrogen atom of Lys195 is in suitable position to form intermolecular H-bond or ionic interaction with the 3-OH (Table 1). Additionally, Asp451 from the IIIA subdomain is able to form intermolecular H-bond with the 4′-OH. It is important to note that the only tryptophan residue of HSA (Trp214) is in close proximity to the benzopyrone moiety of quercetin suggesting the existence of hydrophobic interaction between them (Fig. 8, Table 2). Further, this finding provides a good structural basis to explain the very efficient fluorescence quenching of BSA emission in the presence of quercetin [28]. Also, the model sheds some light on the results obtained by CD displacement experiments. As mentioned, warfarin, the marker ligand of Site I, can displace radiolabelled quercetin from HSA but only at large excess ($c_{querc} = 1.5\ \mu M$, $c_{warf} = 100\ \mu M$) which seems to contradict the high affinity of warfarin for HSA ($K_a \approx 10^5\ M^{-1}$). Our molecular model provides explanation for this virtual discrepancy. Site I is large enough to accommodate both molecules simultaneously and Fig. 9 shows mutual positions of the two ligands. As can be seen, co-binding is possible since the steric interference of bound molecules is only partial and involves the conformationally mobile part of warfarin (the acetonyl and the phenyl groups) while the rigid coumarin moiety fits inside the binding pocket. Similar conclusion can be drawn about sodium salycilate which is even smaller than warfarin and occupies a position distinct from that of quercetin within subdomain IIA.

Table 2
Amino acids of the binding environment of quercetin in HSA obtained from the molecular model

Amino acid residues of the binding site	Closest ring of quercetin	Distance of closest approach (Å)
Leu238	A	2.8
Trp214	A	3.1
Ala291	A	3.1
Leu219	A	3.5
Arg222	A	3.5
Lys199	A	3.8
His242	A	5.5
Asp451	B	2.8
Pro447	B	2.9
Arg218	B	3.8
Cys448	B	4.3
Val343	B	4.6
Ser342	B	5.4
Gln221	B	5.8
Met446	B	5.8
Tyr341	B	5.9
Tyr452	B	5.7
Lys195	C	3.2
Glu292	C	3.5

Residues lying within 6 Å from any of the atoms of quercetin are listed, basic amino acids are italicized.

4. Conclusions

Interaction between the flavonoid, quercetin and human serum albumin was investigated by electronic absorption and circular dichroism spectroscopy. Albumin is the most abundant plasma protein and flavonoids interact with this macromolecule that crucially determines their bioavailability and toxicology. As a result of specific binding of quercetin to HSA, its absorption spectrum is strongly red shifted. This red shift and the decreased absorption intensity suggest that quercetin binds in anionic form in non-planar conformation. Furthermore, due to the asymmetric protein environment, the chirally perturbed electronic

transitions of bound quercetin produce an induced CD spectrum. This was utilized for CD displacement studies with palmitic acid and salicylate to probe the binding site of quercetin. Experiments have suggested that quercetin binds to the IIA subdomain of HSA. The association constant calculated from the induced CD spectra is $1.46 \pm 0.21 \times 10^4\ M^{-1}$. The quercetin binding properties of HSA was also mapped by molecular modelling. Docking calculations found quercetin to be located at Site I of HSA within subdomain IIA in a non-planar conformation. Additionally, the model showed the microenvironment of quercetin to be rich in polar (basic) amino acid residues able to stabilize the negatively charged ligand molecule. Comparison of the positions within the binding cavity of the Site I marker drug warfarin with that of quercetin indicated that these molecules can simultaneously bind by occupying different, partly overlapping rooms within this large hydrophobic pocket.

References

[1] Harborne JB, Williams CA. Advances in flavonoid research since 1992. Phytochemistry 2000;55:481–504.

[2] Cook NC, Samman S. Flavonoids—chemistry, metabolism, cardioprotective effects, and dietary sources. J Nutr Biochem 1996;7:66–76.

[3] Middleton E, Kandaswami C, Theoharides TC. The effects of plant flavonoids on mammalian cells: implications for inflammation, heart disease, and cancer. Pharmacol Rev 2000;52:673–751.

[4] Yang CS, Landau JM, Huang MT, Newmark HL. Inhibition of carcinogenesis by dietary polyphenolic compounds. Annu Rev Nutr 2001;21:381–406.

[5] Solimani R. The flavonols quercetin, rutin and morin in DNA solution: UV-Vis dichroic (and mid-infrared) analysis explain the possible association between the biopolymer and a nucleophilic vegetable-dye. Biochim Biophys Acta 1997;1336:281–94.

[6] Kitson TM, Kitson KE, Moore SA. Interaction of sheep liver cytosolic aldehyde dehydrogenase with quercetin, resveratrol and diethylstilbestrol. Chem-Biol Interact 2001;130:57–69.

[7] Martin-Cordero C, Lopez-Lazaro M, Pinero J, Ortiz T, Cortes F, Ayuso MJ. Glucosylated isoflavones as DNA topoisomerase II poisons. J Enzym Inhib 2000;15:455–60.

[8] Dangles O, Dufour C, Manach C, Morand C, Remesy C. Binding of flavonoids to plasma proteins. Method Enzymol 2001;335:319–33.

[9] Carter DC, Ho JX. Structure of serum albumin. Adv Protein Chem 1994;45:153–203.

[10] Manach C, Morand C, Texier O, Favier ML, Agullo G, Demigne C, Regerat F, Remesy C. Quercetin metabolites in plasma of rats fed diets containing rutin or quercetin. J Nutr 1995;125:1911–22.

[11] Boulton DW, Walle UK, Walle T. Extensive binding of the bioflavonoid quercetin to human plasma proteins. J Pharm Pharmacol 1998;50:43–9.

[12] Sytnik A, Litvinyuk I. Energy transfer to a proton-transfer fluorescence probe: tryptophan to a flavonol in human serum albumin. Proc Natl Acad Sci USA 1996;93:12959–63.

[13] Dockal M, Carter DC, Ruker F. The three recombinant domains of human serum albumin—structural characterization and ligand binding properties. J Biol Chem 1999;274:29303–10.

[14] Peters T. All about albumin. San Diego (CA): Academic Press; 1996.

[15] Mabry TJ, Markham KR, Thomas MB. The systematic identification of flavonoids. Springer-Verlag: New York; 1970.

[16] Wolfbeis OS, Leiner M, Hochmuth P. Absorption and fluorescence spectra, pK_a, values, and fluorescence lifetimes of monohydroxyflavones and monomethoxyflavones. Ber Bunsenges Phys Chem 1984;88:759–67.

[17] Kumar S, Jain SK, Rastogi RC. An experimental and theoretical study of excited-state dipole moments of some flavones using an efficient solvatochromic method based on the solvent polarity parameter, E-T(N). Spectrochim Acta A 2001;57:291–8.

[18] Agrawal PM, Schneider HJ. Deprotonation induced ^{13}C NMR shifts in phenols and flavonoids. Tetrahedron Lett 1983;24:177–80.

[19] Lévai A. Chiroptical techniques in flavonoid chemistry. In: Farkas L, Gábor M, Kállay F, editors. Flavonoids and bioflavonoids. Proceedings of the Fifth Hungarian Bioflavonoid Symposium, Mátrafüred, Hungary, 25–27 May 1977. Budapest: Akadémiai Kiadó; 1977. p. 295–306.

[20] Braude EA, Sondheimer F, Forbes WF. Steric effects in the electronic spectra of organic compounds. Nature 1954;173:117–9.

[21] Rossi M, Rickles LF, Halpin WA. The crystal and molecular structure of quercetin: a biologically active and naturally occurring flavonoid. Bioorg Chem 1986;14:55–69.

[22] Saidman E, Yurquina A, Rudyk R, Molina MAA, Ferretti FH. Theoretical and experimental study on the solubility, dissolution rate, structure and dipolar moment of flavone in ethanol. J Mol Struct 2002;585:1–13.

[23] Zsila F, Bikádi Z, Simonyi M. Induced chirality upon crocetin binding to human serum albumin: origin and nature. Tetrahedron: Asymmetry 2001;12:3125–37.

[24] Bhattacharya AA, Grune T, Curry S. Crystallographic analysis reveals common modes of binding of medium and long-chain fatty acids to human serum albumin. J Mol Biol 2000;303:721–32.

[25] Petitpas I, Bhattacharya AA, Twine S, East M, Curry S. Crystal structure analysis of warfarin binding to human serum albumin—anatomy of drug site I. J Biol Chem 2001;276:22804–9.

[26] Kragh-Hansen U. Evidence for a large and flexible region of human serum albumin possessing high affinity binding sites for salicylate, warfarin, and other ligands. Mol Pharmacol 1988;34:160–71.

[27] Guharay J, Sengupta B, Sengupta PK. Protein–flavonol interaction: fluorescence spectroscopic study. Proteins 2001;43:75–81.

[28] Dangles O, Dufour C, Bret S. Flavonol–serum albumin complexation. Two-electron oxidation of flavonols and their complexes with serum albumin. J Chem Soc Perkin Trans 2 1999;2:737–44.